THEORETICAL ANALYSIS OF RESONANT WIRELESS POWER TRANSMISSION LINKS COMPOSED OF ELECTRICALLY SMALL LOOPS

Alexandre Robichaud[*], Martin Boudreault, and Dominic Deslandes

CoFaMic Research Center, Université du Québec à Montréal (UQAM), Montréal, Canada

Abstract—This paper presents an analytical method to calculate the scattering parameters of a wireless power transmission link composed of electrically small single loop resonators. The proposed method takes into account all the different couplings in the structure. First, the method is presented and used to find the S-parameters for links composed of circular and rectangular resonators. The model is then used to find the optimal topology for a given transmission distance. Validation of the model is done by comparing its results with experimental measurements. Based on this model, a software used for the design of wireless power transmission links has been developed and is presented. Finally, demonstrations that this model produces excellent results are provided. At resonant frequency, an accuracy better than 2% is reached.

1. INTRODUCTION

WIRELESS POWER TRANSMISSION is an idea that has fascinated generations of researchers. The basic concept was proposed and demonstrated a century ago by Nicola Tesla, who carried out several experiments on wireless power transmission by radio waves [1].

Interestingly, in the last decade, wireless power transmission has again become a field of interest. It enables new applications in several fields including customer's electronics, military, medicine and more. One of the most promising techniques is based on resonant magnetic couplings [2].

The main advantage of this technique compared to a simple inductive coupling is its high efficiency. It has been shown that high

transmission efficiency could be achieved over distances of more than 1 meter with relatively small transmitters.

Several papers have been published on this topic. First, in [3] a technique to analyse Wireless Power Transmission Links (WPTL) was derived using the coupled-mode theory. This method provides a good approximation but its accuracy is too low to be useful for final designs or optimizations. Then, in [4, 5], systems for recharging electrical devices based on WiTricity are proposed. In [4], a comparison between traditional chargers and a charger based on WiTricity is made, and in [5] the issue of misalignments between transmitter and receiver is addressed. Then in [6] the design of WPTL for implantable devices is presented. It provides interesting results concerning the influence of different structural parameters on the efficiency of the link.

The contribution of this paper is to present a novel analytical technique to design WPTLs. This has several advantages: it is faster and easier to implement in an optimization software (like the one presented in this paper) and it has a high accuracy. Indeed, the error at the operating frequency is less than 2%.

The WPTLs discussed in this paper are composed of electrically small resonators made of a single loop inductor in series with a discrete capacitor. These WPTL are in fact two pole filters and can be analysed using the well-known filter theory developed for microwave filters [7].

In Section 2, the theory of WPTL is presented. In Section 3, an analysis is performed to evaluate the impedance matrix of the link. This matrix is then used to extract the S-parameters. In Section 4, the influence of misalignment on transmission efficiency is studied. In Section 5, the WPTL design software is presented and used to find the optimal topology for a given transmission. Finally, in Section 6 an experimental validation is shown.

2. THEORY

Figure 1 shows the proposed WPTL where e is the distance between coupling loops and resonators, c is the transmission distance and r the radius of the coupling loops and resonators. All loops are axially aligned. The transmission of the link is given by [7]:

$$S_{21} = \frac{2}{Q_E} \cdot \frac{jK}{\left(\dfrac{1}{Q_E} + \dfrac{1}{Q} + j\Omega\right)^2 + K^2}, \tag{1}$$

where Ω is the normalized frequency, K the coupling coefficient, Q the unloaded quality factor and Q_E the external quality factor. Neglecting
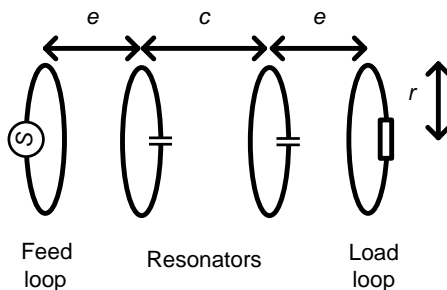
Figure 1. Schematic of the link.

the losses, we can simplify the equation as follows:

$$|S_{21}|_{\Omega=0} = \frac{2KQ_E}{(KQ_E)^2 + 1}. \tag{2}$$

For a lossless transmission where $|S_{21}| = 1$, we obtain the following expression

$$K = \frac{1}{Q_E}. \tag{3}$$

According to (3), the maximum transmission is obtained at the resonant frequency when the external quality factor Q_E is equal to the inverse of K [7, 8]. It is for this reason that the feeding and loading loops are of high importance. Hence, for a given transmission distance, they must be carefully designed and positioned. One can physically move them back and forth in order to find the distance that meets this requirement. This makes the 4-loop design especially interesting and flexible in comparison to the 2 loops design. It should be noted that a 2-loop design could also meet the requirement of (3) if an alternative coupling circuit (capacitors for example) was used. Their transmission efficiency could be identical provided that the coupling circuits have the same losses. However the Q-factor of capacitors is usually smaller than the Q-factor of loops. Hence, coupling using loops generally provides the highest efficiency. If one knows the Q-factor of the capacitors, the efficiency could easily be calculated with the same technique as presented in this paper.

To maximize the transmission, one has to maximize the product of the resonators quality factor and the coupling coefficient, which is defined by:

$$K = \frac{L_{12}}{\sqrt{L_1 L_2}}. \tag{4}$$

Interestingly, K is independent of the resonator's number of turns which means that increasing these would increase Q but not K. Q can be enhanced by enlarging the wire radius. This way, it is thus also possible to achieve comparable transmission efficiency with single loop resonators. The latter presents several advantages, such as ease of fabrication and compactness [8].

The resonators studied in this paper are electrically small and made of a single loop in series with a capacitor. The capacitor value is carefully chosen to obtain the maximum efficiency at the desired frequency. These values are dependant of all the dimensions of the structure, including all coils. The derivation of an analytical technique is then a clear advantage to speed up the design process.

The inductances can be analytically calculated using a magneto-statics technique and the WPTL can be modelled using discrete coupled resonators. Figure 2 shows the equivalent circuit of the latter where, R_2, R_3 and R_4 are the internal resistances of the inductors and R_s and R_e are the resistances of the source and the load respectively. In the equivalent circuit, the first loop corresponds to the feeding loop, the second and third loops correspond to the two resonators and the last loop, to the load loop. Following the procedure given in [9], the transmission coefficient S_{12} and S_{21} are equal and given by:

$$S_{12} = \frac{2R_e \cdot I_2}{V_s}, \tag{5}$$

where the $[S]$ matrix, is the 2×2 scattering matrix of the complete structure, normalized to $50\,\Omega$ and V_s is the feed loop voltage. This equation can be expressed in term of the impedance matrix as:

$$S_{12} = 2R_2 \cdot [Z]_{41}^{-1}. \tag{6}$$
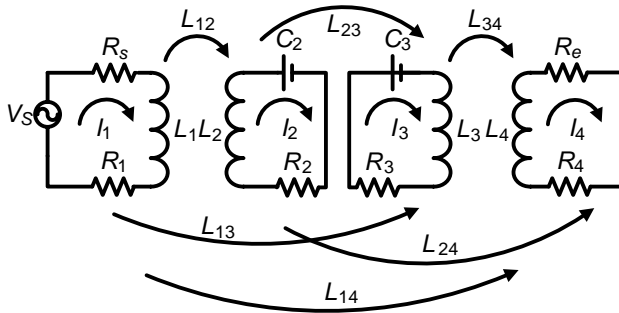
Figure 2. Equivalent circuit of the link.

The reflection coefficient S_{11} is given by:

$$S_{11} = 1 - \frac{2R_e \cdot I_2}{V_s}. \tag{7}$$

The reflection coefficient can also be expressed in term of the impedance matrix as:

$$S_{11} = 1 - 2R_e \cdot [Z]_{11}^{-1}. \tag{8}$$

To determine the impedance matrix of the equivalent circuit, the well-known Kirchhoff's voltage law is applied to each of the four loops. Then, for each loop, the mutual inductance created by the other loops is added. Finally, the equations are written in matrix form and the impedance matrix is extracted:

$$Z = \begin{bmatrix} Z_{11} & -j\omega M_{12} & -j\omega M_{13} & -j\omega M_{14} \\ -j\omega M_{21} & Z_{22} & -j\omega M_{23} & -j\omega M_{24} \\ -j\omega M_{31} & -j\omega M_{32} & Z_{33} & -j\omega M_{34} \\ -j\omega M_{41} & -j\omega M_{42} & -j\omega M_{43} & Z_{44} \end{bmatrix}. \tag{9}$$

In the matrix, Z_{11}, Z_{22}, Z_{33} and Z_{44} are defined as follows,

$$Z_{11} = R_s + R_1 + -j\omega L_1, \tag{10}$$

$$Z_{22} = R_2 + j\omega L_2 + \frac{1}{j\omega C_2 + G_2}, \tag{11}$$

$$Z_{33} = R_2 + j\omega L_2 + \frac{1}{j\omega C_3 + G_3}, \tag{12}$$

$$Z_{44} = R_L + R_4 + j\omega L_4. \tag{13}$$

The first and last terms of the main diagonal correspond to the sum of the resistance and inductive reactance of feeding loop and load loop, respectively. The second and third terms of the main diagonal correspond to the sum of the resistance, inductive reactance and capacitive reactance of the two resonators. Finally, the terms that are not on the main diagonal correspond to the mutual inductances between the loops.

As can be seen, all mutual inductances, which are shown on Figure 2, are considered, i.e., the mutual inductance between loops and resonators, between both resonators, and between both coupling loops. Hence, every significant parameter is considered in the impedance matrix presented in (9).

Therefore, if the value of the inductances and mutual inductances are known, it is possible, using (6), (8) and (9) to calculate exactly the scattering parameters of the link.

3. EVALUATION OF THE IMPEDANCE MATRIX

In this section, the impedance matrix is evaluated analytically for two different geometries, namely the circular loops and the square loops. The procedure detailed in [10] is used to calculate the inductance and the wire resistance is evaluated directly, taking into consideration the skin effect.

3.1. Self and Mutual Inductance of Circular Loops

The loops analyzed in this paper are electrically small. Hence, it is possible to calculate the inductance exactly using the magnetostatics techniques. In the case of a circular loop, the inductance is given by [10]:

$$L_c = \frac{\Psi_{loop}}{I} = \mu_0 \sqrt{a\,(a - r_w)} \left[\left(\frac{2}{k} - k \right) K(k) - \frac{2}{k} E(k) \right], \quad (14)$$

where Ψ is the flux through the loop, I the current in the loop, a the radius of the loop, r_w the radius of the wire, μ_0 the vacuum permeability. K and E are the complete elliptic integral of the first and second kind, and k is given by:

$$k^2 = \frac{4a^2}{(4a^2 + d^2)}. \quad (15)$$

Similarly, the mutual inductance between two loops is given by [10–12]:

$$M_{c,12} = \mu_0 \sqrt{ab} \left[\left(\frac{2}{k} - k \right) K(k) - \frac{2}{k} E(k) \right], \quad (16)$$

where b is the radius of the second loop.

3.2. Self and Mutual Inductance of Rectangular Loops

Similarly, following the procedure detailed in [10], one can find the self and mutual inductances for rectangular loops. For electrically small structures the self-inductance is found using the following equation:

$$\begin{aligned} L_r = \frac{\mu_o}{\pi} \Bigg[&-(l - r_w) \cdot \sinh^{-1}\left(\frac{l - r_w}{w - r_w} \right) - (w - r_w) \cdot \sinh^{-1}\left(\frac{w - r_w}{l - r_w} \right) \\ &+ (l - r_w) \cdot \sinh^{-1}\left(\frac{l - r_w}{r_w} \right) + (w - r_w) \cdot \sinh^{-1}\left(\frac{w - r_w}{r_w} \right) \\ &+ r_w \cdot \sinh^{-1}\left(\frac{r_w}{w - r_w} \right) + r_w \cdot \sinh^{-1}\left(\frac{r_w}{l - r_w} \right) \end{aligned}$$

$$+2\sqrt{(l - r_w)^2 + (w - r_w)^2} - 2\sqrt{(w - r_w)^2 + (r_w)^2}$$

$$-2\sqrt{(l - r_w)^2 + (r_w)^2} - 2r_w \cdot \ln 1 + \sqrt{2} + 2\sqrt{2}r_w \Bigg], \qquad (17)$$

where l is the length and w the width of the loop (as shown in Figure 3).
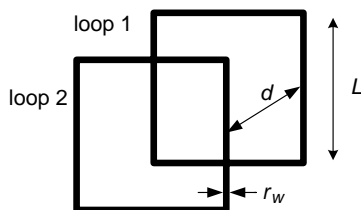
Figure 3. Schematic of the two rectangular loops for mutual inductance calculation.

The mutual inductance between two square loops of side length l_1 and l_2 that are parallel and have their centers aligned can be calculated analytically. To do so, the square loops are split into four pieces of wire and the partial mutual inductance between each pair of wire is calculated. The partial mutual inductance between two parallel wires of same length is given by:

$$M_p(l, r_w, d) = \frac{\mu_0}{2\pi} l \left[\ln\left(\frac{l}{d + r_w} + \sqrt{\left(\frac{l}{d + r_w}\right)^2 + 1} \right) \right.$$

$$\left. -\sqrt{1 + \left(\frac{d + r_w}{l}\right)^2} + \frac{d + r_w}{l} \right], \qquad (18)$$

where l, r_w and d are the length of the wires, the radius of the wire and the shortest distance between the wires, respectively. Based on this expression and using simple geometrical manipulations, we can also calculate the mutual inductance between wires of different length. By doing so for each pair of wires and making the sum of all, we obtain the mutual inductance between two parallel rectangular loops:

$$M_{r,12} = 4\Big[M_p(p + l_2, d_1, r_{w2}) - M_p(p, d_1, r_w2)$$

$$- M_p(p + l_2, d_2, r_{w2}) + M_p(p, d_2, r_{w2}) \Big], \qquad (19)$$

where l_2 is the side length of the biggest loop and l_1 of the smallest, p is given by:

$$p = \frac{l_1 - l_2}{2}, \qquad (20)$$

and d_1 and d_2 are given by:

$$d_1 = \sqrt{\frac{l_1}{2} - \frac{l_2}{2}^2 + d^2}, \tag{21}$$

$$d_2 = \sqrt{\frac{l_1}{2} + \frac{l_2}{2}^2 + d^2}. \tag{22}$$

Hence, using (17) and (19) one can calculate the self and mutual inductance of two square loops.

3.3. Resistance

Finally, the wire resistance of a loop, when considering the skin effect, is given by the Rac-TED-ML [13] formula as follow:

$$R = \frac{L}{\sigma \pi \delta \left(2r - \delta\right)\left(1 + Y\right)}, \tag{23}$$

where σ is the wire conductivity, r is the wire radius, δ is the skin depth and L is equal to $2\pi r$ for the circular coil and equal to $4l$ for the square coil and Y is a correction factor given in [13]. The Rac-TED-ML formula provides accuracy better than 0.09% [13] in comparison with the exact calculation using Kelvin Bessel formula.

In conclusion, for a given link and topology, we can calculate all the self and mutual inductances and resistances present in our model. Then, using (9), the impedance matrix is evaluated.

Finally, using (6) and (8), an accurate evaluation of the scattering parameters is obtained. Hence, for this link, the maximum transmission, bandwidth and other parameters can be analytically calculated and optimized.

4. INFLUENCE OF MISALIGNMENT ON TRANSMISSION EFFICIENCY

Until now we only have considered the case of perfectly aligned resonators. In this section, the influence of misalignment between the resonators is taken into account.

The effect of a misalignment is solely the reduction of the mutual inductance; it does not influence the inductance nor the quality factor of the structures. Hence, its influence can be observed by calculating the variation of the mutual inductance alone.

The mutual inductance between two structures can be calculated using the Neumann integral as follow:

$$M_{12} = \frac{\mu_0}{4\pi} \oint_{c1} \oint_{c2} \frac{dl_1 \cdot dl_2}{R_{12}},\qquad(24)$$

where μ_0 is the vacuum permeability and is equal to $4\pi \cdot 10^{-9}\,\text{H/cm}$. c_1 and c_2, the integral boundaries, are the circumference of the first and second loop, respectively, and R_{12} is the distance between two infinitesimal lengths dl_1 and dl_2. The radius of the wire is considered small compared to the size of the structure. This equation is easily evaluated numerically. Alternatively, although it might be more complex, one can use an analytical approach like the one in [14].

In order to study the effects of lateral misalignment, an initial setup of two perfectly aligned square loops of 10 cm of side length distanced from each other by 10 cm (center-to-center) has been considered (as shown in Figure 4(a)). Then, a parallel translation of one of the loops from -25 cm to $+25$ cm is undertaken while the other structure does not move. The influence of this translation on the mutual inductance is calculated using (24). To validate our calculations, a full wave simulation using HFSS is also performed. The results are shown on Figure 5(a). The agreement between our calculations and the full-wave simulations is excellent. The maximum is obtained when the two structures are perfectly aligned. Also, when the translated structure is moved by one time its diameter (10 cm), the mutual inductance is only reduced by 20%.

In order to study the effects of angular misalignment, the same setup was used (see Figure 4(b)). This time, one loop is rotated on itself while the other structure does not move (for a rotation of zero, the structure are axially aligned). The influence of this rotation on the mutual inductance is calculated using (24) and compared with HFSS
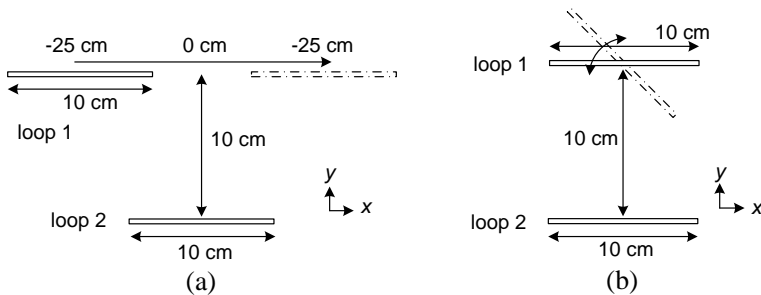
Figure 4. (a) Lateral misalignment. (b) Angular misalignment.
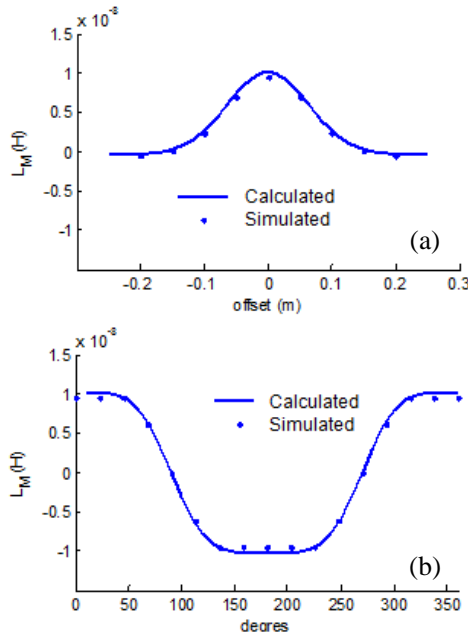
Figure 5. (a) Mutual inductance vs. translation angle for two square resonators with 10 cm side length for a transmission distance of 10 cm. (b) Mutual inductance vs. rotation angle for two square resonators with 10 cm side length and 10 cm transmission distance.

simulations. The results are shown on Figure 5(b). On this figure, one can see that the maximum is reached for perfectly aligned resonators (at 0 and 360 degrees) and that, at 90 degrees, the mutual inductance is zero.

The influence of rotation and translation has been considered. In both cases, one can see that the best transmission is reached when the structures are perfectly aligned. Misalignment results in a reduction of the mutual inductance and, as explained in Section 3, in the transmission efficiency. The proposed technique is very versatile and could be used to evaluate the space region where the power transmission is higher than a certain threshold. For mobile applications, it could also assess the percentage of time that an application is powered wirelessly.

5. OPTIMIZATION OF WPTLS

Now that we have an accurate analytical method to calculate the impedance matrix, it is possible to use it for the optimization of the

structure. Therefore, to facilitate the design of WPTLs, a software called WPTLDesigner was developed using Matlab. Figure 6 shows the software GUI. The software has two main modes of operation. The first one is to calculate the scattering parameters for a given topology. In this mode, the dimensions, the distance between resonators, the distance between resonators and coupling loops, and the values of the capacitors must be specified to the software. Then, the software undertakes the calculation using the analytical method presented in this paper and plots the scattering parameters as a function of the frequency.
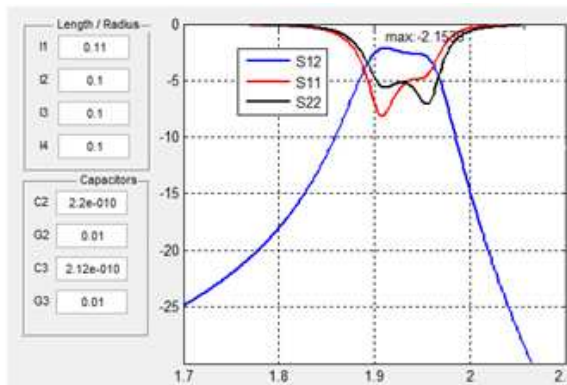
Figure 6. Screenshot of WPTLDesigner.

The second mode gives the possibility of automatic tuning. In this mode, only the frequency of use, the dimensions and the transmission distances must be specified to the software. The software then finds the optimal coupling distance and capacitors values using the presented analytical method in combination with the optimization toolbox of Matlab. Then, it displays the scattering parameters as a function of the frequency.

Now, this software will be used to evaluate the influence of several variables on the efficiency of the link. The influence of the distance between the resonator, the size of the resonator, the frequency and the wire radius will be studied. In order to do so, we will perform three types of optimization: optimization for given distance and frequency but variable resonators size; optimization for given distance and size but variable capacitors and finally, optimization for given distance and frequency but variable wire radius. All optimizations are performed for a link made of square resonators. The results for circular resonators are very similar.

Also, the importance of the three secondary couplings will be analyzed. Theses are the coupling between the loading and feeding

loop, between the first and the third loop and between the second and the fourth loop.

Finally, the importance of the losses in the wire and the capacitors is analyzed.

5.1. Optimization for Given Distance and Frequency but Variable Resonator Size

As a first optimization, the distance between resonators is kept constant while the size of the resonators is varied. Meanwhile, the capacitors are adjusted to keep a constant resonant frequency of 25 MHz. The conductance of the capacitors is calculated using the spice model available on the Website of KEMET Electronic Corporation. Finally, the coupling loops are tuned to reach maximum transmission. This procedure has been applied for five transmission distances ranging from 10 cm to 50 cm. The results are shown on Figure 7(b).

(a)   (b)
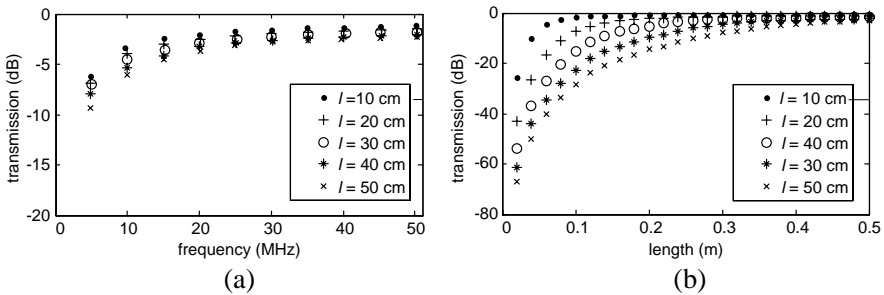
Figure 7. (a) Transmission vs. length of square resonator for a frequency of 25 MHz for a distance of 10 cm to 50 cm. (b) Transmission vs. frequency for 5 resonators size. The frequency is varied by changing the capacitor value.

We can see that the transmission always increases with the size of the resonator. However, it is obvious that for sizes higher than a certain value, corresponding to approximately the transmission distance, enhancement of the transmission becomes negligible. Hence, this fact is capital to finding the best compromise between transmission efficiency and resonator size, and it can be used to design optimal transmission link.

5.2. Optimization for a Given Distance and Size but Variable Frequency

Then, for a given distance and resonator size, the frequency is varied by tuning the capacitors. The conductance of the capacitor is calculated

using the same method as in the last section. Again, the coupling loops are tuned to reach the maximal transmission. Calculations are undertaken for 5 resonator's lengths, ranging from 10 cm to 50 cm. The transmission distance was set to be equal to the length of one side of the resonator.

Figure 7(a) shows the results. It can be seen that the transmission increases with the frequency. The reason is that the required capacitors to reach smaller frequency have higher values and more losses. Hence, the quality factor is smaller which lead to a smaller KQ product and a smaller transmission efficiency.

In conclusion, there is a correlation between the frequency and the transmission efficiency but it is mainly related to the quality factor of the capacitors involved. Hence, the choice of the capacitors for the design of the WPTL is very important.

5.3. Optimization for Given Distance and Frequency but Variable Wire Radius

Finally, for given distance and frequency, the wire radius is varied. Five radiuses, ranging from 0.75 mm to 2 mm, are considered. The wire radius of both resonators and coupling loops are varied. The same tuning was made as for the other optimizations. Also, the distance between the resonators is equal to the resonator side length. Figure 8(a) shows the results.

We can see that the transmission efficiency increases with the wire radius. This can be explained by the fact that a resonator with a larger wire radius has a better quality factor and fewer losses. More
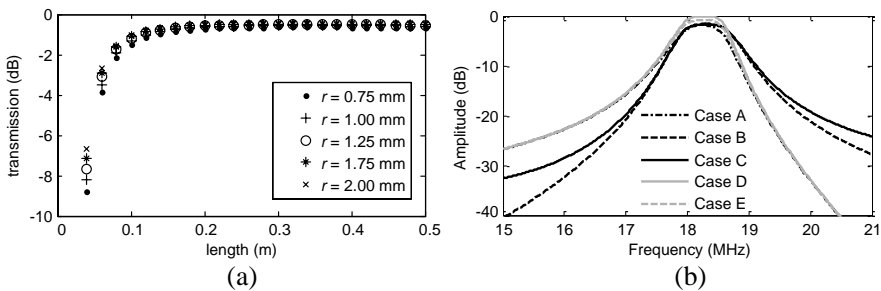
Figure 8. (a) Transmission vs. length of square resonator for a frequency of 25 MHz for wire radius of 0.75 mm to 2 mm. (b) Transmission for different cases. Case A: all couplings and losses are considered; Case B: all secondary coupling are neglected; Case C: coupling between feeding and loading loop is neglected; D: all losses are neglected; E: only the capacitors losses are neglected.

importantly, this effect is less important when reaching the maximum transmission region. The difference between the largest and smallest wire radii, for a length of 20 cm and above, is only of about 0.3 dB. However, if the size of the resonator is kept at a value comparable to that of the transmission distance, as proposed earlier, the wire radius has a significant impact.

5.4. Influence of Secondary Couplings and Losses

An analysis of the importance of the secondary coupling, and of the wire and capacitors losses has been made. Figure 8(b) shows the results.

In Case A, all couplings and losses are considered. To analyse the influence of the secondary coupling, two cases are considered. In Case B, all secondary couplings are neglected. In Case C, only the coupling between the loading and feeding loop is neglected. One can see that the secondary couplings don't have a significant influence on the center frequency. However, they are extremely important outside the passband. They should always be considered for an accurate model over a large frequency band.

To analyze the influence of the losses, two cases are considered. In Case D, all losses are neglected. In Case E, only the capacitor losses are neglected. For both cases, all couplings are considered. One can see that, when all losses are considered, the maximal transmission is equal to 1.4 dB. When the capacitor losses are neglected, the maximal transmission increases to 0.7 dB. Finally, when the wire losses are neglected, it increases to 0 dB (lossless transmission). Hence, in this case, the capacitor and wire losses are each responsible of a loss of efficiency of approximately 7%. Therefore, the choice of low loss capacitor and wire is of first importance.

6. EXPERIMENTAL VALIDATION

Finally, the proposed technique was experimentally validated using inductors made of copper wire with diameter of 1.5 mm and standard

Table 1. Parameters of the measured WPTLs.

	Radius/Length	Capacitor	Frequency
Circle 1	5.5 cm	220 pF	20.1 MHz
Circle 2	7.1 cm	330 pF	14 MHz
Square 1	10.8 cm	220 pF	18.2 MHz
Square 2	14.5 cm	330 pF	12.2 MHz

through-hole capacitors. To measure the transmission, a 2-port network analyzer with standard coaxial cables was used and a calibration was undertaken. The measurement of several topologies of WPTLs were performed and compared with the theoretical calculations. Table 1 shows the details of these tests and Figure 9 and Figure 10 show the results. As for Figure 11, it shows the experimental setup for those validations.

As can be seen, the agreement between the proposed method and the measurement is excellent for all topologies. At the resonant frequency, the difference between calculation and measurement for the transmission is less than 2%. The proposed technique provides accurate results over a wide frequency band. The level of accuracy enables efficient optimization of WPTLs.
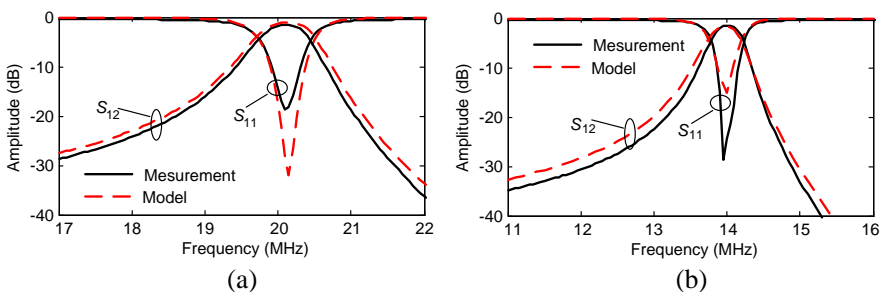
Figure 9. (a) Comparison of calculation and measures for a circular link with a radius of 5 cm and a capacitor value of 220 nF. (b) Comparison of calculation and measures for a circular link with a radius of 7 cm and a capacitor value of 330 nF.
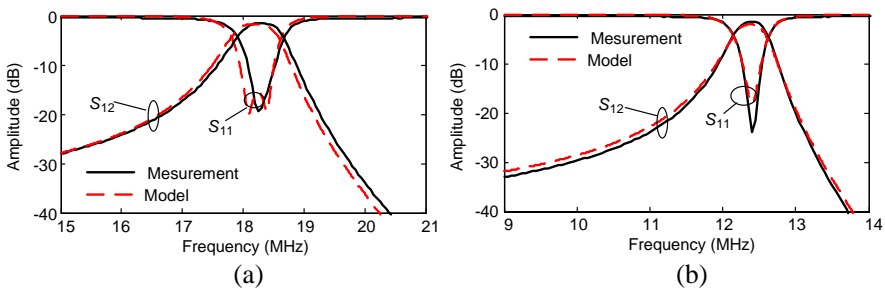
Figure 10. (a) Comparison of calculation and measures for a square link with length size of 10 cm and capacitor value of 220 nF. (b) Comparison of calculation and measures for a square link with length size of 14 cm and capacitor value of 330 nF.
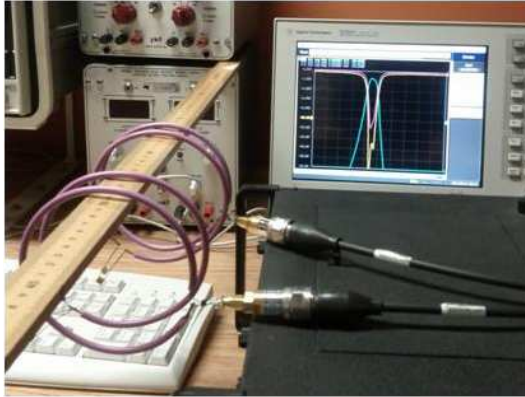
Figure 11. Photo of the physical model.

7. CONCLUSION

This paper presented a novel analytical model for calculating the transmission of a WPTL composed of electrically small single loop resonator. This model predicts, with an accuracy better than 2%, the transmission of WPTLs for different topologies and frequencies.

Furthermore, a software based on the proposed model was developed and presented, which greatly simplifies the design process of WPTLs by allowing their optimization. It is then shown that increasing the size of resonators beyond the transmission distance does not enhance the transmission efficiency significantly. It was also shown that the wire radius has a significant impact on efficiency especially when the transmission distance is similar to the size of the resonators. Finally, it was shown that when the resonators are composed of a single loop with a capacitor, the Q-factor of capacitor has a significant impact on the efficiency of the link. Therefore, they must be carefully chosen to meet the requirement of the designed WPTL.

REFERENCES

1. Tesla, N., "Apparatus for transmitting electrical energy," US Patent 1,119,732, Dec. 1, 1914.
2. Karalis, A., J. D. Joannopoulos, and M. Soljačić, "Efficient wireless non-radiative mid-range energy transfer," *Annals of Physics*, Vol. 323, No. 1, 34–48, Jan. 2008.
3. Kurs, A., A. Karalis, R. Moffatt, J. D. Joannopoulos, P. Fisher, and M. Soljačić, "Wireless power transfer via strongly coupled

magnetic resonances," *Science*, Vol. 317, No. 5834, 83–86, Jun. 2007.

4. Ho, S. L., J. Wang, W. N. Fu, and M. Sun, "A comparative study between novel WiTricity and traditional inductive magnetic coupling in wireless charging," *IEEE Transactions on Magnetics*, Vol. 47, No. 5, 1522–1525, May 2011.

5. Wang, J., S. L. Ho, and W. N. Fu, "Analytical design study of a novel WiTricity charger with lateral and angular misalignments for efficient wireless energy transmission," *IEEE Transactions on Magnetics*, Vol. 47, No. 10, 2616–2619, Oct. 2011.

6. Yin, N., G. Xu, Q. Yang, J. Zhao, X. Yang, J. Jin, W. Fu, and M. Sun, "Analysis of wireless energy transmission for implantable device based on coupled magnetic resonance," *IEEE Transactions on Magnetics*, Vol. 48, No. 2, Feb. 2012.

7. Robichaud, A., M. Boudreault, and D. Deslandes, "Parametric analysis of helical resonators for resonant wireless power transmission links," *IEEE NEWCAS Conference*, 405–408, Jun. 2012.

8. Robichaud, A., M. Boudreault, and D. Deslandes, "Comparison between inductance topologies for resonant wireless power transmission applications," *IEEE Asia-Pacific Microwave Conference Proceedings (APMC)*, 397–399, Dec. 2012.

9. Hong, J.-S. and M. J. Lancaster, *Microstrip Filters for RF/Microwave Applications*, 235–272, John Wiley & Sons, New York, NY, 2001.

10. Paul, C., *Inductance: Loop and Partial,* John Wiley & Sons, New Jersey, 2010.

11. Mutashar, S., M. A. Hannan, A. S. Salina, and A. Hussain, "Design of spiral circular coils in wet and dry tissue for bio-implanted micro-system applications," *Progress In Electromagnetic Research M*, Vol. 32, 181–200. 2013.

12. Maxwell, J. C., *A Treatise on Electricity and Magnetism, Volume II*, Clarendon Press, Oxford, 1873.

13. Knight, D. W., "Practical continuous functions and formulae for the internal impedance of cylindrical conductors," Mar. 2010, http://www.g3ynh.info/zdocs/comps/Zint.pdf.

14. Babic, S., F. Sirois, C. Akyel, and C. Girardi, "Mutual inductance calculation between circular filaments arbitrarily positioned in space: Alternative to Grover's formula," *IEEE Transactions on Magnetics*, Vol. 46, No. 9, 3591–3600, Sep. 2010.